Work fluctuations for a Brownian particle driven by a correlated external random force

Arnab Pal and Sanjib Sabhapandit
Raman Research Institute, Bangalore 560080, India
(Received 24 July 2014; published 11 November 2014)

We have considered the underdamped motion of a Brownian particle in the presence of a correlated external random force. The force is modeled by an Ornstein-Uhlenbeck process. We investigate the fluctuations of the work done by the external force on the Brownian particle in a given time interval in the steady state. We calculate the large deviation functions as well as the complete asymptotic form of the probability density function of the performed work. We also discuss the symmetry properties of the large deviation functions for this system. Finally we perform numerical simulations and they are in a very good agreement with the analytic results.

DOI: 10.1103/PhysRevE.90.052116 PACS number(s): 05.40.−a, 05.70.Ln

I. INTRODUCTION

In recent times the fluctuation theorem (FT) has generated a great deal of excitement in the field of nonequilibrium statistical mechanics, as it allows thermodynamic concepts to be applied to also small systems, as well as to systems that are arbitrarily far from equilibrium. The FT expresses universal properties of the probability density function (PDF) $p(\Omega)$ for functional $\Omega[x(\tau)]$, such as work, heat, power flux, or entropy production, evaluated along the fluctuating trajectories $x(\tau)$ taken from ensembles with well-specified initial distributions. There have been a number of theoretical [2–28] and experimental [29–39] studies to elucidate different aspects of FT. We refer to the recent review [1] which contains an extensive list of references both from the theoretical and the experimental aspects.

The FT can be broadly classified into two groups, namely, the transient FT (TFT) and the steady-state FT (SSFT). The TFT pioneered by Evans and Searles [2] applies to relaxation towards a steady state but at finite time. In this work, they obtain the symmetries of the PDF of "entropy production" at the transient. On the other hand the SSFT quantifies the "entropy production" Ω_τ, in a time duration τ, in the nonequilibrium steady state as

$$\frac{p(\Omega_\tau = \omega\tau)}{p(\Omega_\tau = -\omega\tau)} \sim e^{\tau\omega}. \tag{1}$$

This was first found by Evans *et al.* in simulations of two-dimensional sheared fluids [3] and then proven by Gallavotti and Cohen [4,5] using assumptions about chaotic dynamics. Kurchan [6] and Lebowitz and Spohn [7] have established this theorem for stochastic diffusive dynamics. In all these early works, the total entropy production has been identified with the entropy production in the medium. However, it was shown in [8] that the SSFT holds even for finite times in the steady state if one incorporates the entropy production of the system in the total entropy production. Though the FT for total entropy production has been found to be robust under rather general conditions, it is not so universal for the observables such as work, heat, power, etc. [9–12,14–17,20–26]. While the FT, as given in Eq. (1), deals only with the symmetry properties of the probability distributions, it does not offer a detailed description of the full probability distributions. Therefore, one is also interested in going beyond FT and characterizing the stochastic properties of these observables in detail. The reason that these observables are mostly accompanied by non-Gaussian fluctuations rather than the Gaussian one makes the computation of these distributions highly nontrivial and only a few cases are available where one can do so [22–26]. The long-time behavior of the PDF is often expressed in terms of the the so-called large deviation function (LDF) [41], and in the recent years, many efforts have been devoted to the computation of LDFs in nontrivial models [18,19]. In this paper, we study such a model system, which can be experimentally realizable, and the work fluctuations can be investigated in great detail.

Another important feature of this paper is to study the effects of stochastic driving in work statistics. There have been several works to understand the effect of deterministic driving, such as constant dragging, linear and nonlinear time dependent forcing, sinusoidal oscillations, nonconserving driving, anisotropic shear flow, applying an electric field or a magnetic field, etc., on work statistics. Surprisingly, only a few attempts have been made on the issue of "stochastic driving" [22,23,26]. Stochastic driving is an issue which raises interest both conceptually and on practical purposes. The conceptual barrier lies on the very nature of the stochastic driving: What kinds of drivings are feasible? Is the stochasticity reversible or irreversible by nature? How much entropy production is then associated with the driving? Second, absolute deterministic driving is a hypothetical concept in an experimental setup. Any kind of deterministic driving will be always accompanied by minute fluctuations and thus it is very important to take them into account [40].

In this article, we consider an underdamped Brownian particle driven by a correlated random external field. We study the PDF of the work done by the external random field in a given duration. The exact LDF associated with the PDF is found to have a nontrivial form and a nontrivial dependence on the driving parameter. The SSFT corresponding to the work fluctuations is found to be held in a restrictive parameter space of the model, confirming the fact that the FT for work and heat is nongeneric although the SSFT total entropy production remains unaffected.

The paper is organized as follows. In the following section, we define the model. In Sec. III we compute the moment-generating function (MGF) of work W_τ performed in a given time τ in steady state, which has the form $\langle e^{-\lambda W_\tau}\rangle \sim g(\lambda)e^{\tau\mu(\lambda)}$. In Sec. IV, we invert the MGF to obtain the asymptotic form (for large τ) of the PDF of the work.

We discuss the symmetry properties of the large deviation functions and its connection with the FT in Sec. V. Finally we conclude in Sec. VI. Some details of the calculation has been relegated to the Appendix.

II. MODEL

Consider a Brownian particle of mass m, in the presence of an external fluctuating time-dependent field, at a temperature T. The velocity $v(t)$ of the particle evolves according to the underdamped Langevin equation, given by

$$m\frac{dv}{dt}+\gamma v=f(t)+\eta_1, \tag{2}$$

where γ is the friction coefficient. The viscous relaxation time scale for the particle is $\tau_\gamma=m/\gamma$. The thermal noise η_1 is taken to be a Gaussian white noise with mean zero and correlation$\langle\eta_1(t)\eta_1(s)\rangle=2D\delta(t-s)$, where diffusion constant $D=\gamma k_BT$ and k_B is the Boltzmann constant. The external stochastic field f is modeled by an Ornstein-Uhlenbeck process,

$$\frac{df}{dt}=-\frac{f}{\tau_0}+\eta_2, \tag{3}$$

where η_2 is another Gaussian white noise with mean zero and correlation $\langle\eta_2(t)\eta_2(s)\rangle=2A\delta(t-s)$. This system reaches a steady state and in the steady state the external force has zero mean and covariance $\langle f(t)f(s)\rangle=A\tau_0\exp(-|t-s|/\tau_0)$.

The heat current flowing from the bath to the particle is the force exerted by the bath times the velocity of the particle [42]. Therefore, in a given time τ, the total amount of heat flow (in units of K_BT) is given by

$$Q_\tau=\frac{1}{k_BT}\int_0^\tau(-\gamma v+\eta_1)v(t)dt. \tag{4}$$

On the other hand, the change in the internal energy of the particle in this finite interval τ is given by

$$\Delta U(\tau)=\frac{1}{k_BT}\left[\frac{1}{2}mv^2(\tau)-\frac{1}{2}mv^2(0)\right]. \tag{5}$$

Then the first law of the thermodynamics (conservation of energy) gives $\Delta U(\tau)=W_\tau+Q_\tau$, where W_τ is the work done on the particle by the external force, which is given by

$$W_\tau=\frac{1}{k_BT}\int_0^\tau f(t)v(t)dt. \tag{6}$$

This work is a stochastic quantity and our goal is to compute its PDF $P(W_\tau)$.

It will prove convenient to introduce the following two dimensionless parameters:

$$\theta=\frac{\tau_0^2A}{D}\quad\text{and}\quad\delta=\frac{\tau_0}{\tau_\gamma}. \tag{7}$$

Effects of stochastic modulation on the work statistics will be quantified in term of these two parameters.

III. MOMENT-GENERATING FUNCTION

We begin by writing Eqs. (2) and (3) in the matrix form

$$\frac{dU}{dt}=-AU+B\eta, \tag{8}$$

where $U=(v,f)^T$ and $\eta=(\eta_1,\eta_2)^T$ are column vectors, and A and B are 2×2 matrices given by

$$A=\begin{pmatrix}1/\tau_\gamma & -1/m\\ 0 & 1/\tau_0\end{pmatrix},\quad B=\begin{pmatrix}1/m & 0\\ 0 & 1\end{pmatrix}. \tag{9}$$

To compute the PDF of W_τ, we first consider its moment-generating function, constrained to fixed initial and final configurations U_0 and U, respectively:

$$Z(\lambda,U,\tau|U_0)=\langle e^{-\lambda W_\tau}\delta[U-U(\tau)]\rangle_{U_0}, \tag{10}$$

where the averaging is over the histories of the thermal noises starting from the initial condition U_0 and λ is the conjugate variable. It is easy to show that this restricted moment-generating function satisfies the Fokker-Planck equation

$$\frac{\partial Z}{\partial\tau}=\mathscr{L}_\lambda Z, \tag{11}$$

with the initial condition $Z(\lambda,U,0|U_0)=\delta(U-U_0)$. The Fokker-Planck operator is given by

$$\mathscr{L}_\lambda=\frac{D}{m^2}\frac{\partial^2}{\partial v^2}+\frac{D\theta}{\tau_0^2}\frac{\partial^2}{\partial f^2}+\frac{1}{\tau_\gamma}\frac{\partial}{\partial v}v+\frac{1}{\tau_0}\frac{\partial}{\partial f}f -\frac{f}{m}\frac{\partial}{\partial v}-\frac{\lambda\gamma}{D}fv. \tag{12}$$

The solution of this equation can be formally expressed in the eigenbases of the operator $\mathscr{L}_\lambda$ and the large-τ behavior is dominated by the term containing the largest eigenvalue. Thus, for large τ, one can write

$$Z(\lambda,U,\tau|U_0)=\chi(U_0,\lambda)\Psi(U,\lambda)e^{\tau\mu(\lambda)}+\cdots, \tag{13}$$

where $\mu(\lambda)$ is the largest eigenvalue and $\Psi(U,\lambda),\chi(U,\lambda)$ are the corresponding right and left eigenfunctions of the Fokker-Planck operator $\mathscr{L}_\lambda$. Then, $\mathscr{L}_\lambda\Psi(U,\lambda)=\mu(\lambda)\Psi(U,\lambda)$ and $\int dU\,\chi(U,\lambda)\Psi(U,\lambda)=1$ from the orthonormal condition of the eigenfunctions. Following the detailed calculation given in the Appendix, we find that

$$\mu(\lambda)=\frac{1}{2\tau_\gamma}[1-\bar{\nu}(\lambda)], \tag{14a}$$

where

$$\bar{\nu}(\lambda)=\frac{1}{\delta}[\sqrt{1+\delta^2+2\delta\nu(\lambda)}-1], \tag{14b}$$

with

$$\nu(\lambda)=\sqrt{1+4\theta\lambda(1-\lambda)}. \tag{14c}$$

We note that $\mu(\lambda)$ obeys the so-called Gallavotti-Cohen symmetry, $\mu(\lambda)=\mu(1-\lambda)$.

Computation of the largest eigenvalue and the eigenfunctions in this problem relies on the "finite-time Fourier transform" method developed in [20,22,23] since the direct diagonalization is a formidable task here. On the other hand, scenarios dealing with systems having a bounded configuration space (such as energy or particle exchanging lattice exclusion models, multilevel systems with finite energy states), one deals with a finite-dimensional Markov evolution operator for which several diagonalization methods (e.g., Ferrari method) are available. A few such instances of computing the largest eigenvalues for discrete finite state systems are discussed in the literature [18,19,25,26].

That said, the moment-generating function can now be obtained by averaging the restricted generating function over the initial variables U_0 with respect to the steady-state distribution $P_{SS}(U_0)$ and integrating out the the final variables U,

$$Z(\lambda,\tau) = \int dU \int dU_0 P_{SS}(U_0) Z(\lambda,U,\tau|U_0), \tag{15}$$

where $P_{SS}(U_0) = \Psi(U_0,0)$. This yields

$$Z(\lambda,\tau) = \langle e^{-\lambda W_\tau}\rangle = g(\lambda)e^{\tau\mu(\lambda)} + \cdots, \tag{16}$$

where

$$g(\lambda) = \int dU \int dU_0 \Psi(U_0,0)\chi(U_0,\lambda)\Psi(U,\lambda). \tag{17}$$

The full forms of $\Psi(U,\lambda)$ and $\chi(U_0,\lambda)$ are given by Eq. (A31). Using these we find the $g(\lambda)$ as given by Eqs. (A35) and (A36) in the Appendix.

IV. PROBABILITY DISTRIBUTION FUNCTION

The PDF $P(W_\tau)$ is related to the moment-generating function $Z(\lambda,\tau)$ as

$$P(W_\tau) = \frac{1}{2\pi i}\int_{-i\infty}^{+i\infty} Z(\lambda,\tau)e^{\lambda W_\tau} d\lambda, \tag{18}$$

where the integration is done in the complex λ plane. Inserting the large-τ form of $Z(\lambda,\tau)$ given by Eq. (16), we obtain

$$P(W_\tau = w\tau/\tau_\gamma) \approx \frac{1}{2\pi i}\int_{-i\infty}^{+i\infty} g(\lambda)e^{(\tau/\tau_\gamma) f_w(\lambda)} d\lambda, \tag{19}$$

where

$$f_w(\lambda) = \tfrac{1}{2}[1 - \bar{\nu}(\lambda)] + \lambda w. \tag{20}$$

In the large-τ limit, we can use the saddle-point approximation, in which one chooses the contour of integration along the steepest descent path through the saddle point λ^*. The saddle point can be obtained solving the equation

$$f_w'(\lambda^*) = 0, \tag{21}$$

or equivalently,

$$\bar{\nu}'(\lambda^*) = 2w. \tag{22}$$

The above equation yields

$$\theta(1-2\lambda^*) = w\nu(\lambda^*)\sqrt{1+\delta^2+2\delta\nu(\lambda^*)}. \tag{23}$$

Since θ, δ, and $\nu(\lambda)$ are always positive, it is clear that $\mathrm{sgn}(1-2\lambda^*) = \mathrm{sgn}(w)$. The above equation can be simplified to the cubic form

$$\nu^3(\lambda^*) + a\nu^2(\lambda^*) - b = 0, \tag{24}$$

where

$$a = \frac{\theta + (1+\delta^2)w^2}{2\delta w^2}, \tag{25a}$$

$$b = \frac{\theta+\theta^2}{2\delta w^2}. \tag{25b}$$

We observe that one of the roots of the cubic equation for $\nu(\lambda^*)$ is real while the other two are complex. Equation (23) suggests the root to be real, and it is given by

$$\nu(\lambda^*) = -\frac{a}{3}[1 - (1+2k+3\sqrt{3lk})^{-1/3} - (1+2k+3\sqrt{3lk})^{1/3}], \tag{26a}$$

where $l = b/a^3$ and $k = (27/4)l - 1$. Note that $l > 0$. Therefore, $\nu(\lambda^*)$ is evidently real for $k > 0$. On the other hand, when $k < 0$, it can be simplified to the evidently real form

$$\nu(\lambda^*) = -\frac{a}{3}[1 - 2\cos(\phi/3)], \tag{26b}$$

where $\phi = \tan^{-1}[3\sqrt{3l|k|}/(1+2k)] \in [0,\pi]$.

In the limit $w \to \pm\infty$, from Eq. (25) we have, $a \to (1+\delta^2)/(2\delta)$ and $b \to 0$. Therefore, $l \to 0$ and $k \to -1$, giving $\phi \to \pi$. This yields $\nu(\lambda^*) \to 0$. On the other hand, for $w \to 0$, we have $a \sim \theta/(2\delta w^2)$. Using this we find that $\nu(\lambda^*) \to \sqrt{1+\theta}$. It is also evident as Eq. (23) gives $\lambda^* = 1/2$ for $w = 0$, and then, from Eq. (14c), we get $\nu(1/2) = \sqrt{1+\theta}$.

Now using Eq. (23), the saddle point $\lambda^*(w)$ can be expressed in terms of $\nu(\lambda^*)$. Therefore, the function $f_w(\lambda)$ at the saddle point λ^* can be expressed in terms of $\nu(\lambda^*)$, and is given by

$$\begin{aligned} h_s(w) &:= f_w(\lambda^*) \\ &= \frac{1}{2}\left[\frac{1}{\delta} + 1 + w\right] \\ &\quad - \frac{1}{2}\left[\frac{1}{\delta} + \frac{w^2}{\theta}\nu(\lambda^*)\right]\sqrt{1+\delta^2+2\delta\nu(\lambda^*)}. \end{aligned} \tag{27}$$

To find the region in which λ^* lies, it is useful to express $\nu(\lambda)$ in the form

$$\nu(\lambda) = \sqrt{4\theta(\lambda_+ - \lambda)(\lambda - \lambda_-)}, \tag{28}$$

where

$$\lambda_\pm = \tfrac{1}{2}[1 \pm \sqrt{1+\theta^{-1}}]. \tag{29}$$

Clearly, $\nu(\lambda)$ has two branch points on the real-λ line at $\lambda_\pm$. Moreover, it is real and positive in the (real) interval $\lambda \in (\lambda_-,\lambda_+)$. Since $\lambda_+ - \lambda_- = \sqrt{1+\theta^{-1}}$, as $\lambda \to \lambda_\pm$, we have $\nu(\lambda) \to 2[\theta(1+\theta)]^{1/4}|\lambda - \lambda_\pm|^{1/2}$. Therefore, from Eq. (23) we get

$$w \to \mp \frac{[\theta(1+\theta)]^{1/4}}{2\sqrt{1+\delta^2}}|\lambda^* - \lambda_\pm|^{-1/2} \quad \text{as} \quad \lambda^* \to \lambda_\pm. \tag{30}$$

In other words, $\lambda^*(w)$ merges to $\lambda_\pm$ as one takes the limit $w \to \mp\infty$. This also agrees with the observation that $\nu(\lambda^*) \to 0$ as $|w| \to \infty$. For any finite w the saddle point $\lambda^* \in (\lambda_-,\lambda_+)$. In Fig. 1 we plot the saddle point λ^* as a function of w using Eq. (23).

Now, if $g(\lambda)$ is analytic in the range $\lambda \in (0,\lambda^*)$, we can deform the contour along the path of the steepest descent through the saddle point, and obtain $P(W_\tau)$ using the usual

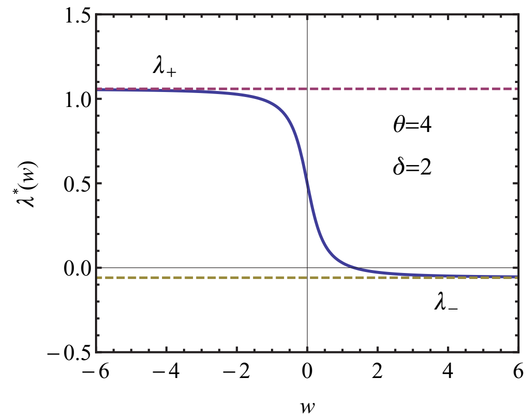

FIG. 1. (Color online) The behavior of λ^* is shown (solid line) as a function of w, for a set of parameters $\theta = 4, \delta = 2$, which merges to $\lambda_\pm$ (dashed lines) as $w \to \mp\infty$.

saddle-point method. However, more sophistication is needed when $g(\lambda)$ contains singularities. Therefore it is essential to analyze $g(\lambda)$ for possible singularities.

We first recall $g(\lambda)$ from Eqs. (A35) and (A36),

$$g(\lambda) = [f_1(\lambda,\theta,\delta)]^{-1/2}[f_2(\lambda,\theta,\delta)]^{-1/2}. \tag{31}$$

Following the Appendix, we also recall that $f_1(\lambda,\theta,\delta)$ does not change its sign and always stays positive in the region $[\lambda_-,\lambda_+]$. This is not the case for $f_2(\lambda,\theta,\delta)$. While $f_2(\lambda,\theta,\delta) > 0$ for $\lambda_- \leqslant \lambda \leqslant 0$, in some region in the (θ,δ) space, $f_2(\lambda_+,\theta,\delta) < 0$. Therefore, in that (θ,δ) region, $f_2(\lambda,\theta,\delta)$ must have a zero at some intermediate $\lambda = \lambda_0 > 0$, which gives rise to a branch-point singularity in $g(\lambda)$. Figure 2 shows parameter region in which $g(\lambda)$ possesses a singularity. The phase boundary between the region in which $g(\lambda)$ has a singularity and the singularity-free region is given by the equation $f_2(\lambda_+,\theta,\delta)$=0. In the limit $\delta \to 0$ we get $\theta \to 1/3$.

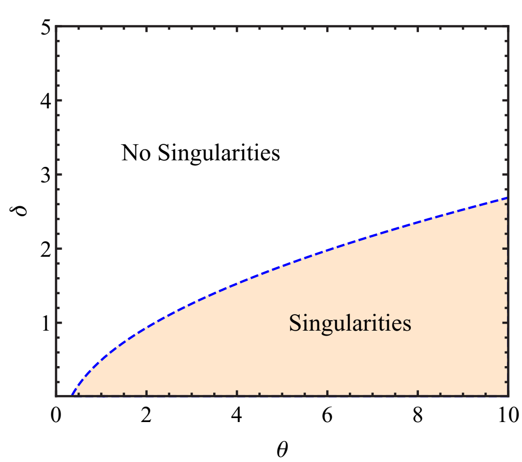

FIG. 2. (Color online) This plot depicts the analytic properties of $g(\lambda)$. In the shaded region of the (θ,δ) plane, $g(\lambda)$ possesses a singularity, where $f_2(\lambda_+,\theta,\delta) < 0$. On the other hand, in the unshaded region $g(\lambda)$ does not have any singularities, where $f_2(\lambda_+,\theta,\delta) > 0$. These two domains are separated by the boundary given by the equation $f_2(\lambda_+,\theta,\delta) = 0$.

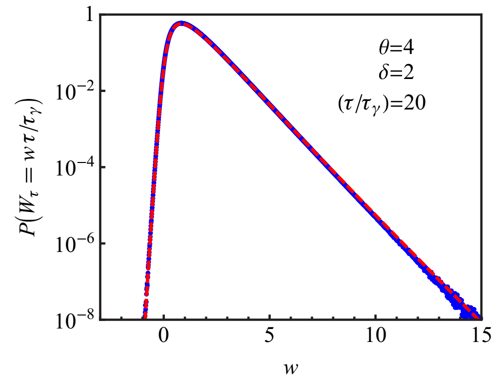

FIG. 3. (Color online) The (red) dashed line plots the analytical result of $P(W_\tau)$ against the scaled variable $w = W_\tau/(\tau/\tau_\gamma)$, while the (blue) points are numerical simulation results.

A. Case of no singularities

In the singularity-free region (Fig. 2), the asymptotic PDF of the work done is obtained using the standard saddle-point method, which gives

$$P(W_\tau = w\tau/\tau_\gamma) \approx \frac{g(\lambda^*)e^{\frac{\tau}{\tau_\gamma}h_s(w)}}{\sqrt{2\pi\frac{\tau}{\tau_\gamma}f_w''(\lambda^*)}}, \tag{32}$$

where $h_s(w)$ is given by Eq. (27) and

$$f_w''(\lambda^*) = -\frac{\bar{\nu}''(\lambda^*)}{2} = \frac{2}{\nu(\lambda^*)}\frac{\theta + w^2[1+\delta^2+3\delta\nu(\lambda^*)]}{[1+\delta^2+2\delta\nu(\lambda^*)]^{1/2}}, \tag{33}$$

which is expressed in terms of w and $\nu(\lambda^*)$ given by Eq. (26). Figure 3 shows a very good agreement between the analytic result given by Eq. (32) and numerical simulations.

B. Case of a singularity

For a given value of δ and θ, the location of the branch point λ_0 is fixed between the origin and λ_+. On the other hand, the saddle point λ^* increases monotonically along the real-λ line from λ_- to λ_+ as w decreases from $+\infty$ to $-\infty$. For sufficiently large w, the saddle-point lies in the interval (λ_-,λ_0) and therefore the contour of integration can be deformed into the steepest-descent path, which passes through the saddle point, without touching λ_0. However, as w decreases, the saddle point hits the branch point at some specific value $w = w^*$ given by

$$\lambda^*(w^*) = \lambda_0. \tag{34}$$

For $w < w^*$, the steepest-descent contour wraps around the branch cut between λ_0 and λ^*. We here present the results for both regimes $w < w^*$ and $w > w^*$ respectively, applying the method developed in [23].

1. $w > w^*$

For $w > w^*$, the contour is deformed through the saddle point without touching the singularity and we obtain

$$P(W_\tau = w\tau/\tau_\gamma) \approx \frac{g(\lambda^*)e^{\frac{\tau}{\tau_\gamma}h_s(w)}}{\sqrt{2\pi\frac{\tau}{\tau_\gamma}f_w''(\lambda^*)}} R_1\left(\sqrt{\frac{\tau}{\tau_\gamma}[h_0(w)-h_s(w)]}\right), \quad (35)$$

where $f_w''(\lambda^*)$ is given by Eq. (33) and the function $R_1(z)$ is given by

$$R_1(z) := \frac{z}{\sqrt{\pi}} e^{z^2/2} K_{1/4}(z^2/2), \quad (36)$$

with $K_{1/4}(z)$ being the modified Bessel function of the second kind.

2. $w < w^*$

For $w < w^*$, the contribution comes from both the branch point and the saddle point; i.e.,

$$P(W_\tau) \approx P_B(W_\tau) + P_S(W_\tau), \quad (37)$$

where the branch point contribution is

$$P_B(W_\tau = w\tau/\tau_\gamma) \approx \frac{\tilde{g}(\lambda_0)e^{\frac{\tau}{\tau_\gamma}h_0(w)}}{\sqrt{\pi\frac{\tau}{\tau_\gamma}|f_w'(\lambda_0)|}} R_2\left(\sqrt{\frac{\tau}{\tau_\gamma}[h_0(w)-h_s(w)]}\right), \quad (38)$$

where

$$h_0(w) := f_w(\lambda_0) = \frac{1}{2}[1-\bar{\nu}(\lambda_0)] + \lambda_0 w, \quad (39)$$

$$f_w'(\lambda_0) = -\frac{\bar{\nu}'(\lambda_0)}{2} + w, \quad (40)$$

$$\tilde{g}(\lambda_0) = \lim_{\lambda\to\lambda_0} |\sqrt{\lambda-\lambda_0}\, g(\lambda)|, \quad (41)$$

and

$$R_2(z) = \sqrt{\frac{2z}{\pi}} \int_0^z \frac{1}{\sqrt{u}} e^{-2zu+u^2} du. \quad (42)$$

The contribution coming from the saddle point is given by

$$P_S(W_\tau = w\tau/\tau_\gamma) \approx \frac{|g(\lambda^*)|e^{\frac{\tau}{\tau_\gamma}h_s(w)}}{\sqrt{2\pi\frac{\tau}{\tau_\gamma}|f_w''(\lambda^*)|}} R_4\left(\sqrt{\frac{\tau}{\tau_\gamma}[h_0(w)-h_s(w)]}\right), \quad (43)$$

where the function $R_4(z)$ is given by

$$R_4(z) = \sqrt{\frac{\pi}{2}} z e^{z^2/2}[I_{-1/4}(z^2/2) + I_{1/4}(z^2/2)] - \frac{4z}{\pi}\,{}_2F_2(1/2,1;3/4,5/4;z^2), \quad (44)$$

and $I_{\pm 1/4}(z)$ are modified Bessel functions of the first kind and ${}_2F_2(a_1,a_2;b_1,b_2;z)$ is the generalized hypergeometric function. We again find a very good agreement between the analytical results and numerical simulations; see Fig. 4.

In the following we analyze the $\delta = 0$ case, which becomes a special case of the problem of a single Brownian particle connected with two heat baths at different temperatures studied by Visco [16]. Here, we obtain the PDF.

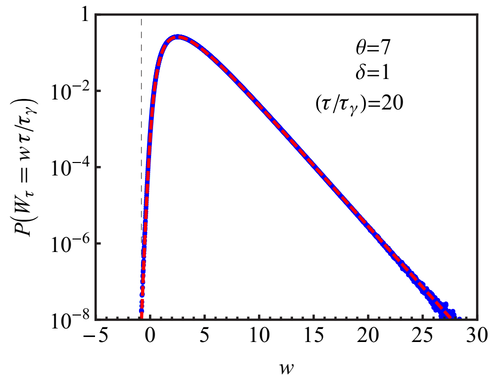

FIG. 4. (Color online) The (red) dashed line plots the analytical result for $P(W_\tau)$, while the (blue) points are numerical simulation results. The vertical dashed line marks the position of the singularity $w^* = -0.801661...$ for the values of $\theta = 7, \delta = 1$.

C. $\delta = 0$

We first note that $g(\lambda)$ takes a simple form in the limit $\delta \to 0$, given by

$$g(\lambda) = \frac{\sqrt{2\nu}}{\sqrt{\nu+1+2\lambda\theta}} \frac{\sqrt{2}}{\sqrt{\nu+1-2\lambda\theta}}. \quad (45)$$

It is easy to show [22] that $g(\lambda)$ is completely analytic for $\theta \leqslant 1/3$, and the PDF is obtained using the saddle-point method as

$$P(W_\tau = w\tau/\tau_\gamma) \approx \frac{g(\lambda^*)e^{\frac{\tau}{\tau_\gamma}h_s(w)}}{\sqrt{2\pi\frac{\tau}{\tau_\gamma}f_w''(\lambda^*)}}, \quad (46)$$

where the second derivative of $f_w(\lambda)$ along the real-λ axis at λ^* is given by [22]

$$f_w''(\lambda^*) = \frac{2(w^2+\theta)^{3/2}}{\sqrt{\theta(1+\theta)}} \quad (47)$$

and

$$h_s(w) := f_w(\lambda^*) = \frac{1}{2}\left[1 + w - \sqrt{w^2+\theta}\sqrt{1+\frac{1}{\theta}}\right]. \quad (48)$$

On the other hand, if $\theta > 1/3$, it is easy to show that $g(\lambda)$ picks up a branch point singularity at $\lambda = \lambda_0 = 2/(1+\theta)$, which corresponds to [22]

$$w^* = \frac{\theta(\theta-3)}{3\theta-1}. \quad (49)$$

Then one needs to perform a contour integration avoiding the branch cut as mentioned in the last section. For $w > w^*$, using the same prescription [23], we find the PDF as

$$P(W_\tau = w\tau/\tau_\gamma) \approx \frac{g(\lambda^*)e^{\frac{\tau}{\tau_\gamma}h_s(w)}}{\sqrt{2\pi\frac{\tau}{\tau_\gamma}f_w''(\lambda^*)}} R_1\left(\sqrt{\frac{\tau}{\tau_\gamma}[h_0(w)-h_s(w)]}\right), \quad (50)$$

where

$$h_0(w) := f_w(\lambda_0) = \frac{1-\theta}{1+\theta} + \frac{2w}{1+\theta}. \quad (51)$$

For $w < w^*$, the contribution to the PDF comes both from the saddle and the branch point,

$$P(W_\tau) \approx P_B(W_\tau) + P_S(W_\tau), \tag{52}$$

where the branch point contribution is

$$P_B(W_\tau = w\tau/\tau_\gamma) \approx \frac{\tilde{g}(\lambda_0) e^{\frac{\tau}{\tau_\gamma} h_0(w)}}{\sqrt{\pi \frac{\tau}{\tau_\gamma} |f'_w(\lambda_0)|}} R_2\left(\sqrt{\frac{\tau}{\tau_\gamma}[h_0(w) - h_s(w)]}\right), \tag{53}$$

where

$$\tilde{g}(\lambda_0) = \frac{3\theta - 1}{2\theta\sqrt{2(1+\theta)}}, \quad f'_w(\lambda_0) = w - w^*, \tag{54}$$

and the function $R_2(z)$ is given by Eq. (42). The contribution coming from the saddle point is given by

$$P_S(W_\tau = w\tau/\tau_\gamma) \approx \frac{|g(\lambda^*)| e^{\frac{\tau}{\tau_\gamma} h_s(w)}}{\sqrt{2\pi \frac{\tau}{\tau_\gamma} |f''_w(\lambda^*)|}} R_4\left(\sqrt{\frac{\tau}{\tau_\gamma}[h_0(w) - h_s(w)]}\right), \tag{55}$$

where the function $R_4(z)$ is given by Eq. (44). Figure 5 compares the analytical results with the numerical simulations.

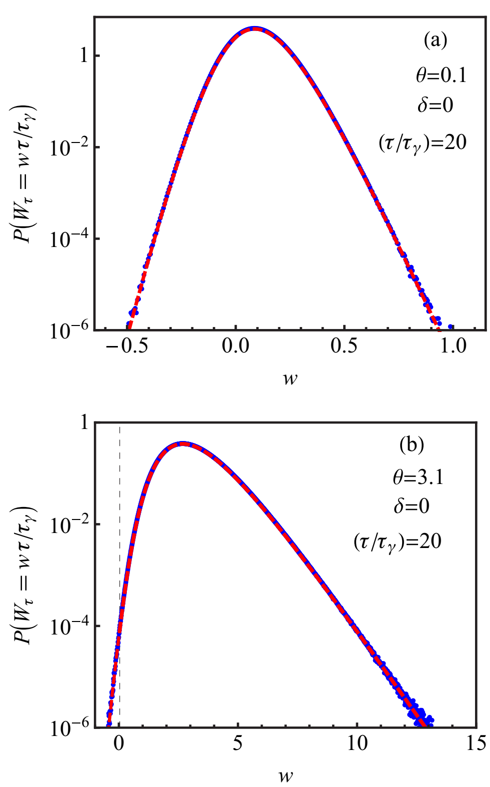

FIG. 5. (Color online) The (red) dashed lines plot analytical results for $P(W_\tau)$, while the (blue) points are numerical simulation results, for the $\delta = 0$ case. The vertical dashed line in (b) marks the position of the singularity which is $w^* = 0.037...$ in this case.

V. LARGE DEVIATION FUNCTION AND THE FLUCTUATION THEOREMS

The LDF, associated with the PDF, is defined as

$$h(w) = \lim_{(\tau/\tau_\gamma)\to\infty} \frac{1}{(\tau/\tau_\gamma)} \ln P(W_\tau = w\tau/\tau_\gamma). \tag{56}$$

Due to the large deviation form of the PDF, $P(W_\tau = w\tau/\tau_\gamma) \sim e^{(\tau/\tau_\gamma)h(w)}$, the FT given by Eq. (1) is equivalent to the following symmetry relation of the LDF:

$$h(w) - h(-w) = w. \tag{57}$$

Now, in the parameter region where $g(\lambda)$ is analytic (see Fig. 2), the LDF is given by $h(w) = h_s(w)$. In this case, it is clear from Eq. (27) that the above symmetry relation (57) holds, as $\nu(\lambda^*)$ is an even function of w.

On the other hand, in the parameter region where $g(\lambda)$ has a singularity, the LDF is given by

$$h(w) = \begin{cases} h_s(w) & \text{for} \quad w > w^*, \\ h_0(w) & \text{for} \quad w < w^*. \end{cases} \tag{58}$$

Therefore, it is evident that if $w^* < 0$, the symmetry relation (57) holds only in the specific range $w^* < w < -w^*$. Otherwise, it fails to satisfy. Nevertheless, even for $w > w^*$, one still gets a linear relation $h(w) - h(-w) = 2\lambda_0 w$, in the range $w \in (-w^*, w^*)$.

The physical origin of the singularities can be understood by examining the moment-generating function $Z(\lambda) = \langle e^{-\lambda\Omega}\rangle \sim g(\lambda)e^{\tau\mu(\lambda)}$. The prefactor $g(\lambda)$ is computed by integrating out the relevant degrees of freedom at the final time and at the initial time suitably averaging over the initial condition. Whenever the PDF $P(\Omega)$ has an *exponential* tail, the integral $\int_{-\infty}^{\infty} e^{-\lambda\Omega} P(\Omega)\, d\Omega$ diverges for some specific value of λ, which manifests as a singularity in the complex λ plane. The value of λ where the singularity arises indeed gives the decay rate of $P(\Omega)$.

VI. SUMMARY

In this paper, we have discussed an underdamped Brownian particle driven by an external correlated stochastic force, modeled by an Ornstein-Uhlenbeck process. We have studied the probability density function (PDF) of the work done W_τ on the particle by the external random force, in a given time τ. The behavior can be characterized in terms of two dimensionless parameters, namely, (i) θ, which gives the relative strength between the external random force and the thermal noise, and (ii) δ, which characterizes the ratio between the viscous relaxation time and the correlation time of the external force. In the large-τ limit, we have obtained the moment-generating function (MGF) in the form $\langle e^{-\lambda W_\tau}\rangle \sim g(\lambda)e^{\tau\mu(\lambda)}$. While $\mu(\lambda)$ is analytic in the relevant region of λ (where the saddle point lies), the prefactor $g(\lambda)$ shows analytical as well as singular behavior in different parts of the parameter space spanned by (θ,δ). We have obtained the PDF in both analytic and nonanalytic regions of (θ,δ) space, by carefully inverting the MGF. The entire analytical results have been supported by numerical simulations. In the limit $\delta \to 0$, our model becomes a special case of a problem of a single Brownian particle coupled to two distinct reservoirs, first proposed by Derrida and Brunet [43] and later studied by Visco [16].

We have also looked at the validity of the fluctuation theorem (FT) for work, in terms of the symmetry properties of the large deviation function. We have found that in the (θ,δ) region where $g(\lambda)$ is analytic, the FT is satisfied. On the other hand, in the nonanalytic region, the symmetry of the large deviation function breaks down. In particular, the PDF picks up an exponential tail characterized by the singularity and this leads to the violation of the steady-state fluctuation theorems.

Finally, we have provided a nontrivial example where the exact LDF as well as the complete asymptotic form of the PDF of the work done by a correlated stochastic force can be computed.

ACKNOWLEDGMENTS

The authors thank the Galileo Galilei Institute for Theoretical Physics, Florence, Italy, for the hospitality and the INFN for partial support during the completion of this work. S.S. acknowledges the support of the Indo-French Centre for the Promotion of Advanced Research under Project No. 4604-3.

APPENDIX: DETAILED CALCULATION OF THE MGF

We recall Eqs. (8) and (9),

$$\frac{dU}{dt} = -AU + B\eta, \tag{A1}$$

where $U = (v,f)^T$ and $\eta = (\eta_1,\eta_2)^T$ are column vectors and A, B are 2×2 matrices given by

$$A = \begin{pmatrix} 1/\tau_\gamma & -1/m \\ 0 & 1/\tau_0 \end{pmatrix}, \quad B = \begin{pmatrix} 1/m & 0 \\ 0 & 1 \end{pmatrix}. \tag{A2}$$

The expression for W_τ can then be expressed in terms of these matrices,

$$W_\tau = \frac{\gamma}{2D}\int_0^\tau dt U^T A_1 U, \tag{A3}$$

where A_1 is a real symmetric matrix

$$A_1 = \begin{pmatrix} 0 & 1 \\ 1 & 0 \end{pmatrix}. \tag{A4}$$

Using the integral representation of the delta function, we rewrite the moment-generating function

$$Z(\lambda,U,\tau|U_0) = \int \frac{d^2\sigma}{(2\pi)^2} e^{i\sigma^T U}\langle e^{-\lambda W_\tau - i\sigma^T U(\tau)}\rangle_{U,U_0}. \tag{A5}$$

Now, we proceed by defining the finite-time Fourier transforms and inverses as follows:

$$[\tilde{U}(\omega_n),\tilde{\eta}(\omega_n)] = \frac{1}{\tau}\int_0^\tau dt[U(t),\eta(t)]\exp(-i\omega_n t), \tag{A6a}$$

$$[U(t),\eta(t)] = \sum_{n=-\infty}^{\infty}[\tilde{U}(\omega_n),\tilde{\eta}(\omega_n)]\exp(i\omega_n t), \tag{A6b}$$

with $\omega_n = 2\pi n/\tau$.

In the frequency domain, the Gaussian noise configurations denoted by $\{\eta(t): 0 < t < \tau\}$ can be well described by the infinite sequence $\{\tilde{\eta}(\omega_n): n = -\infty,\ldots,-1,0,+1,\ldots,\infty\}$ of Gaussian random variables having the following correlations:

$$\langle\tilde{\eta}(\omega)\tilde{\eta}^T(\omega')\rangle = \frac{2D}{\tau}\delta(\omega+\omega')\mathrm{diag}\big(1,\theta/\tau_0^2\big). \tag{A7}$$

The Fourier transform of $U(t)$ is then straightforward and henceforth the expression for W_τ becomes

$$\begin{aligned}\tilde{U} &= GB\tilde{\eta} - \frac{1}{\tau}G\Delta U W_\tau \\ &= \frac{\gamma\tau}{2D}\sum_{n=-\infty}^{\infty}\tilde{U}^T(\omega_n)A_1\tilde{U}^*(\omega_n),\end{aligned} \tag{A8}$$

where $G(\omega) = (i\omega I + A)^{-1}$ and $\Delta U = U(\tau) - U(0)$, with I being the identity matrix. The elements of G are $G_{11} = \tau_\gamma(i\omega\tau_\gamma + 1)^{-1}, G_{22} = \tau_0(i\omega\tau_0 + 1)^{-1}, G_{12} = G_{11}G_{22}/m$, $G_{21} = 0$. Substituting $\tilde{U}$ from the above expression in W_τ and grouping the negative indices into their positive counterparts, we obtain

$$\begin{aligned}W_\tau = {}& \frac{\gamma\tau}{2D}\bigg[\tilde{\eta}_0^T\big(BG_0^T A_1 G_0 B\big)\tilde{\eta}_0 - \frac{2}{\tau}\Delta U^T\big(G_0^T A_1 G_0 B\big)\tilde{\eta}_0 \\ &+ \frac{1}{\tau^2}\Delta U^T\big(G_0^T A_1 G_0\big)\Delta U\bigg] \\ &+ \frac{\gamma\tau}{D}\sum_{n=1}^{\infty}\bigg[\tilde{\eta}^T(BG^T A_1 G^* B)\tilde{\eta}^* \\ &- \frac{1}{\tau}\Delta U^T(G^T A_1 G^* B)\tilde{\eta}^* - \frac{1}{\tau}\tilde{\eta}^T(BG^T A_1 G^*)\Delta U \\ &+ \frac{1}{\tau^2}\Delta U^T(G^T A_1 G^*)\Delta U\bigg],\end{aligned} \tag{A9}$$

where $G_0 = G(\omega = 0) = A^{-1}, \tilde{\eta}_0 = \tilde{\eta}(0)$. The finite time Fourier series can be written for $U(\tau)$ as well:

$$\begin{aligned}U(\tau) &= \lim_{\varepsilon\to 0}\sum_{n=-\infty}^{\infty}\tilde{U}(\omega_n)e^{-i\omega_n\varepsilon} \\ &= \lim_{\varepsilon\to 0}\sum_{n=-\infty}^{\infty}\left(GB\tilde{\eta} - \frac{1}{\tau}G\Delta U\right)e^{-i\omega_n\varepsilon} \\ &= \lim_{\varepsilon\to 0}\sum_{n=-\infty}^{\infty}(GB\tilde{\eta})e^{-i\omega_n\varepsilon},\end{aligned} \tag{A10}$$

where we observe that $\tau^{-1}\sum_n G(\omega_n)e^{-i\omega_n\varepsilon} = 0$ for large τ. This is because while converting the summation into an integral we note that all the poles of $G(\omega)$ lie in the upper half plane. In other words, the function $G(\omega)$ is analytic in the lower half. Using this expression we obtain

$$\begin{aligned}\sigma^T U(\tau) = {}& \sigma^T G_0 B\tilde{\eta}_0 + \sum_{n=1}^{\infty}[e^{-i\omega_n\varepsilon}\tilde{\eta}^T(BG^T\sigma) \\ &+ e^{i\omega_n\varepsilon}(\sigma^T G^* B)\tilde{\eta}^*].\end{aligned} \tag{A11}$$

The average quantity then can be rewritten as

$$\langle e^{-\lambda W_\tau - i\sigma^T U(\tau)}\rangle = \prod_{n=0}^{\infty}\langle e^{s_n}\rangle, \tag{A12}$$

where

$$s_n = -\lambda\tau\tilde{\eta}^T c_n \tilde{\eta}^* + \tilde{\eta}^T \alpha_n + \alpha_{-n}^T \tilde{\eta}^* - \frac{\lambda}{\tau}\frac{\gamma}{D}\Delta U^T (G^T A_1 G^*)\Delta U \quad \text{for} \quad n \geqslant 1 \tag{A13}$$

and

$$s_0 = -\frac{\lambda\tau}{2}\tilde{\eta}_0^T c_0 \tilde{\eta}_0 + \alpha_0^T \tilde{\eta}_0 - \frac{\lambda}{2\tau}\frac{\gamma}{D}\Delta U^T\left(G_0^T A_1 G_0\right)\Delta U, \tag{A14}$$

in which we have used the following definitions:

$$c_n = \frac{\gamma}{D} B G^T A_1 G^* B, \tag{A15}$$

$$\alpha_n = \lambda\frac{\gamma}{D}(B G^T A_1 G^*)\Delta U - i e^{-i\omega_n \varepsilon} B G^T \sigma. \tag{A16}$$

We can now calculate the average $\langle e^{s_n}\rangle$ independently for each $n \geqslant 1$ with respect to the Gaussian PDF $P(\tilde{\eta}) = \pi^{-2}(\det\Lambda)^{-1}\exp(-\tilde{\eta}^T\Lambda^{-1}\tilde{\eta}^*)$ with $\Lambda^{-1} = \frac{2D}{\tau}\mathrm{diag}(1,\theta/\tau_0^2)$, which gives

$$\langle e^{s_n}\rangle = \frac{\exp\left[\alpha_{-n}^T\Omega_n^{-1}\alpha_n - \frac{\lambda}{\tau}\frac{\gamma}{D}\Delta U^T(G^T A_1 G^*)\Delta U\right]}{\det(\Lambda\Omega_n)}, \tag{A17}$$

where $\Omega_n = \lambda\tau c_n + \Lambda^{-1}$. Similarly, calculating the average of $n = 0$ term with respect to the Gaussian PDF $P(\tilde{\eta}_0) = (2\pi)^{-1}(\det\Lambda)^{-1/2}\exp(-\frac{1}{2}\tilde{\eta}_0^T\Lambda^{-1}\tilde{\eta}_0)$, we get

$$\langle e^{s_0}\rangle = \frac{\exp\left[\frac{1}{2}\alpha_0^T\Omega_0^{-1}\alpha_0 - \frac{\lambda}{2\tau}\frac{\gamma}{D}\Delta U^T\left(G_0^T A_1 G_0^*\right)\Delta U\right]}{\sqrt{\det(\Lambda\Omega_0)}}. \tag{A18}$$

The restricted moment-generating function can now be rewritten as

$$Z(\lambda,U,\tau|U_0) = \int \frac{d^2\sigma}{(2\pi)^2} e^{i\sigma^T U}\prod_{n=0}^{\infty}\langle e^{s_n}\rangle, \tag{A19}$$

where using the fact $\langle e^{s_n}\rangle = \langle e^{s_{-n}}\rangle$, we can write

$$\prod_{n=0}^{\infty}\langle e^{s_n}\rangle = \exp\left(-\frac{1}{2}\sum_{n=-\infty}^{\infty}\ln[\det(\Lambda\Omega_n)]\right)\exp\left(\frac{1}{2\tau}\sum_{n=-\infty}^{\infty}\left[\alpha_{-n}^T\tau\Omega_n^{-1}\alpha_n - \lambda\frac{\gamma}{D}\Delta U^T G^T A_1 G^*\Delta U\right]\right). \tag{A20}$$

The determinant in Eq. (A20) is found to be

$$\det(\Lambda\Omega_n) = 1 + \frac{4\theta\lambda(1-\lambda)}{\tau_0^2\tau_\gamma^2}|G_{11}|^2|G_{22}|^2. \tag{A21}$$

Now in large-τ limit, we can replace the summations over n into an integral over ω; i.e., $\sum_n \to \tau\int\frac{d\omega}{2\pi}$. The first part of the summation is then

$$\tau\mu(\lambda) = -\frac{\tau}{2}\int\frac{d\omega}{2\pi}\ln\{\det[\Lambda\Omega(\omega)]\}, \tag{A22}$$

where $\mu(\lambda)$ is given by Eq. (14a). Similarly, the second part of the summation can be converted into an integral. Finally, after doing some manipulations, we obtain

$$\prod_{n=0}^{\infty}\langle e^{s_n}\rangle \approx e^{\tau\mu(\lambda)}\exp\left[-\frac{1}{2}\sigma^T H_1\sigma + i\Delta U^T H_2\sigma + \frac{1}{2}\Delta U^T H_3\Delta U\right], \tag{A23}$$

in which we have defined the following matrices:

$$H_1 = \int_{-\infty}^{\infty}\frac{d\omega}{2\pi}G^* B(\tau\Omega^{-1})BG^T, \tag{A24}$$

$$H_2 = -\lim_{\varepsilon\to 0}\frac{\lambda}{2\pi}\frac{\gamma}{D}\int_{-\infty}^{\infty}d\omega e^{i\omega\varepsilon}G^+ A_1 G B(\tau\Omega^{-1})^* BG^+, \tag{A25}$$

and

$$H_3 = -\frac{\lambda}{2\pi}\frac{\gamma}{D}\int_{-\infty}^{\infty}d\omega G^T A_1 G^* + \frac{\lambda^2}{2\pi}\frac{\gamma^2}{D^2}\int_{-\infty}^{\infty}d\omega G^T A_1 G^* B(\tau\Omega^{-1})BG^T A_1 G^*. \tag{A26}$$

We then evaluate the matrices by performing the integral by the method of contours. For convenience, we write down the elements of the matrices respectively:

$$H_1^{11} = \frac{D\tau_\gamma}{m^2}\frac{1}{1+\delta\bar{\nu}}\left(\delta + \frac{1+\theta}{\nu}\right), \tag{A27a}$$

$$H_1^{12} = H_1^{21} = \frac{D\theta}{m}\frac{1-2\lambda}{\nu(1+\delta\bar{\nu})}, \tag{A27b}$$

$$H_1^{22} = \frac{D\theta}{\tau_0}\frac{1}{1+\delta\bar{\nu}}\left(1+\frac{\delta}{\nu}\right). \tag{A27c}$$

The elements of the H_2 matrix are

$$H_2^{11} = \frac{1}{\nu(1+\delta\bar{\nu})}\left[\lambda\theta + \frac{1}{2}(1-\nu) + \frac{1}{2}\delta\nu(1-\bar{\nu})\right], \tag{A28a}$$

$$H_2^{12} = -\frac{\lambda\gamma\theta}{\nu(1+\delta\bar{\nu})}, \tag{A28b}$$

$$H_2^{21} = -\frac{\lambda\delta}{\gamma\nu(1+\delta\bar{\nu})} + \frac{\delta(1-\nu)}{2\gamma\nu(1+\delta\bar{\nu})}, \tag{A28c}$$

$$H_2^{22} = \frac{\delta(1-\nu\bar{\nu})}{2\nu(1+\delta\bar{\nu})}. \tag{A28d}$$

The elements of the H_3 matrix are given by

$$H_3^{11} = \frac{\lambda^2\theta\gamma^2\tau_\gamma}{D\nu(1+\delta\bar{\nu})}, \tag{A29a}$$

$$H_3^{12} = H_3^{21} = \frac{\lambda\gamma\tau_\gamma(\bar{\nu}-\nu)}{2D\nu(1+\delta\bar{\nu})} \times \frac{\delta(1+\nu)+(1+\delta\bar{\nu})(\delta-\delta\bar{\nu}-2)}{[1+\delta\bar{\nu}-\delta-\nu]}. \tag{A29b}$$

$$H_3^{22} = -\frac{\lambda(1-\lambda)\delta\tau_0}{D\nu(1+\delta\bar{\nu})}. \tag{A29c}$$

We note that the matrices H_1 and H_3 are symmetric and they satisfy the relation $H_3 = (I+H_2)H_1^{-1}H_2^T$. Inserting Eq. (A23) into Eq. (A19) and performing the Gaussian integral over σ, we obtain

$$Z(\lambda,U,\tau|U_0) \approx \frac{e^{\tau\mu(\lambda)}}{2\pi\sqrt{\det(H_1(\lambda))}} e^{-\frac{1}{2}U^T L_1(\lambda)U} e^{-\frac{1}{2}U_0^T L_2(\lambda)U_0}, \tag{A30}$$

where $L_1(\lambda) = H_1^{-1}(I+H_2^T)$ and $L_2(\lambda) = -H_1^{-1}H_2^T$. We immediately identify the right and left eigenfunctions respectively as

$$\Psi(U,\lambda) = \frac{1}{2\pi\sqrt{\det(H_1(\lambda))}} \exp\left[-\frac{1}{2}U^T L_1(\lambda)U\right], \tag{A31a}$$

$$\chi(U_0,\lambda) = \exp\left[-\frac{1}{2}U_0^T L_2(\lambda)U_0\right]. \tag{A31b}$$

It is then straightforward to verify $\mathscr{L}_\lambda\Psi(U,\lambda) = \mu(\lambda)\Psi(U,\lambda)$ and $\int dU\,\chi(U,\lambda)\Psi(U,\lambda) = 1$. The steady-state distribution is given by

$$\begin{aligned} P_{SS}(U) &= Z(\lambda=0,U,\tau\to\infty|U_0) \\ &= \Psi(U,\lambda=0) \\ &= \frac{1}{2\pi\sqrt{\det(H_1(0))}} \exp\left[-\frac{1}{2}U^T L_1(0)U\right], \end{aligned} \tag{A32}$$

where $L_1(0)$ and given by

$$L_1(0) = \frac{1}{\det H_1(0)} \frac{D}{1+\delta} \begin{pmatrix} \frac{\theta}{\tau_0}(1+\delta) & -\frac{\theta}{m} \\ -\frac{\theta}{m} & \frac{\tau_\gamma}{m^2}(1+\delta+\theta) \end{pmatrix}. \tag{A33}$$

It is worth noting that the deviation of the system from equilibrium can also be measured using Eq. (A32):

$$\alpha = \frac{\langle v^2\rangle_{ss}}{\langle v^2\rangle_{eq}} - 1, \tag{A34}$$

where $\langle v^2\rangle_{ss}$ is the velocity variance in the steady state which can be found from Eq. (A33) and $\langle v^2\rangle_{eq}$ is that of in equilibrium in the absence of the external driving. Hence, one finds $\alpha = \theta/(1+\delta)$.

Now, averaging the restricted generating function with respect to the steady-state distribution $P_{SS}(U)$, we get back Eq. (16), where $g(\lambda)$ is given by

$$\begin{aligned} g(\lambda) &= \left[\det\left(I+H_2^T\right)\right]^{-1/2} \\ &\quad\times\left\{\det\left[I-H_1(0)H_1^{-1}(\lambda)H_2^T(\lambda)\right]\right\}^{-1/2}, \end{aligned} \tag{A35}$$

where the first and second terms are due to tracing out the final and initial variables, respectively. Using the forms of the matrices given by Eqs. (A27) and (A28), we obtain

$$\begin{aligned} f_1(\lambda,\theta,\delta) &:= \det\left(I+H_2^T\right) \\ &= \frac{1}{4\nu(1+\delta\bar{\nu})^2}[p(\lambda)+2\theta\lambda q(\lambda)], \end{aligned} \tag{A36a}$$

$$\begin{aligned} f_2(\lambda,\theta,\delta) &:= \det\left[I-H_1(0)H_1^{-1}(\lambda)H_2^T(\lambda)\right] \\ &= \frac{1}{4(1+\delta)^2}\frac{1}{\theta+(1+\delta\bar{\nu})^2}[r(\lambda)+2\theta\lambda s(\lambda)], \end{aligned} \tag{A36b}$$

where

$$p(\lambda) = 2+2\nu+\delta(1+\bar{\nu})(1+\delta+3\nu+\delta\nu\bar{\nu}), \tag{A37a}$$

$$q(\lambda) = 2+\delta(\bar{\nu}-1) = 1+\sqrt{1+\delta^2+2\delta\nu}-\delta, \tag{A37b}$$

and

$$\begin{aligned} r(\lambda) &= 2\theta(1+\nu)+2(1+\nu)(1+\delta)^2+[\theta+(1+\delta)^2] \\ &\quad\times[\delta(1+\bar{\nu})^2+\delta(1+\bar{\nu})(1+\delta\bar{\nu})(\nu+\bar{\nu})], \end{aligned} \tag{A38a}$$

$$\begin{aligned} s(\lambda) &= -[2+2\theta+3\theta\delta+\delta\bar{\nu}+\theta\delta\bar{\nu}] \\ &\quad+[\delta+2\delta^2(2+\bar{\nu})+\delta^3(1+3\bar{\nu})]. \end{aligned} \tag{A38b}$$

Let us now analyze the functions $f_1(\lambda,\theta,\delta)$ and $f_2(\lambda,\theta,\delta)$ in detail. We note that the prefactors outside the square brackets of $f_1(\lambda,\theta,\delta)$ and $f_2(\lambda,\theta,\delta)$ are always positive. Moreover, $p(\lambda)$ and $q(\lambda)$ are again clearly positive in the region $\lambda\in[\lambda_-,\lambda_+]$. In particular, they take the minimum values at $\lambda_\pm$, given by $p(\lambda_\pm) = 2+a_1$ and $q(\lambda_\pm) = 1+a_2 = 2-a_3$, where $a_1 = (1+\delta)(\delta+\sqrt{1+\delta^2}-1)\geqslant 0$, $1\geqslant a_2 = \sqrt{1+\delta^2}-\delta > 0$, and $1 > a_3 = (1+\delta)-\sqrt{1+\delta^2}\geqslant 0$. Therefore, $f_1(\lambda_+,\theta,\delta) > 0$ as $\lambda_+ > 0$. On the other hand, at $\lambda=\lambda_-$ we get

$$\begin{aligned} p(\lambda_-)+2\theta\lambda_- q(\lambda_-) &= (2+a_1)+2\theta\lambda_-(2-a_3) \\ &= a_1+(-2a_3\theta\lambda_-)+2(1+2\theta\lambda_-). \end{aligned}$$

The first two summands in the last line of the above expression are clearly positive (note that $\lambda_- < 0$). Moreover, it can be shown that

$$1+2\theta\lambda_- = \sqrt{1+\theta}[\sqrt{1+\theta}-\sqrt{\theta}] > 0. \tag{A39}$$

This also implies that

$$1+2\theta\lambda > 0 \quad \text{for} \quad \lambda\in[\lambda_-,\lambda_+]. \tag{A40}$$

Therefore, $f_1(\lambda_-,\theta,\delta) > 0$, which implies that $f_1(\lambda,\theta,\delta)$ stays positive in the region $\lambda\in[\lambda_-,\lambda_+]$.

Similarly, we can analyze the second term $f_2(\lambda,\theta,\delta)$. Clearly, $r(\lambda)$ is always positive in the region $\lambda \in [\lambda_-,\lambda_+]$. On the other hand, the first line in the expression of $s(\lambda)$ given by Eq. (A38b) is negative whereas the second line is positive; $s(\lambda)$ can take both positive and negative values in the (θ,δ,λ) space. Writing Eq. (A38b) as $s(\lambda) = -b_1 + b_2$ with both $b_1 > 0$ and $b_2 > 0$, we get

$$r(\lambda) + 2\theta\lambda s(\lambda) = [r(\lambda) - b_2] + (1 + 2\theta\lambda)b_2 + (-2b_1\theta\lambda).$$

By explicitly expanding $r(\lambda)$, it can be seen that all the terms appearing in b_2 completely cancel with some of the terms of $r(\lambda)$. Therefore, $r(\lambda) - b_2 > 0$ for $\lambda \in [\lambda_-,\lambda_+]$. Similarly, according to Eq. (A40), the second summand is positive. Finally, the last summand is clearly positive for $\lambda < 0$. Therefore, $f_2(\lambda,\theta,\delta) > 0$ for $\lambda_- \leqslant \lambda \leqslant 0$.

At $\lambda = \lambda_+$, we find that $r(\lambda_+) + 2\theta\lambda_+ s(\lambda_+)$ changes sign in the parameter space of (θ,δ). The phase boundary that separates the two regions where this function stays positive and negative respectively is given by

$$f_2(\lambda_+,\theta,\delta) = 0, \tag{A41}$$

which is shown in Fig. 2.

[1] U. Seifert, Rep. Prog. Phys. **75**, 126001 (2012).
[2] D. J. Evans and D. J. Searles, Phys. Rev. E **50**, 1645 (1994).
[3] D. J. Evans, E. G. D. Cohen, and G. P. Morriss, Phys. Rev. Lett. **71**, 2401 (1993).
[4] G. Gallavotti and E. G. D. Cohen, Phys. Rev. Lett. **74**, 2694 (1995); J. Stat. Phys. **80**, 931 (1995).
[5] G. Gallavotti, Phys. Rev. Lett. **77**, 4334 (1996).
[6] J. Kurchan, J. Phys. A: Math. Gen. **31**, 3719 (1998).
[7] J. L. Lebowitz and H. Spohn, J. Stat. Phys. **95**, 333 (1999).
[8] U. Seifert, Phys. Rev. Lett. **95**, 040602 (2005).
[9] J. Farago, J. Stat. Phys. **107**, 781 (2002).
[10] R. van Zon and E. G. D. Cohen, Phys. Rev. Lett. **91**, 110601 (2003); Phys. Rev. E **67**, 046102 (2003); **69**, 056121 (2004).
[11] R. van Zon, S. Ciliberto, and E. G. D. Cohen, Phys. Rev. Lett. **92**, 130601 (2004).
[12] O. Mazonka and C. Jarzynski, arXiv:cond-mat/9912121.
[13] O. Narayan and A. Dhar, J. Phys. A **37**, 63 (2004).
[14] M. Baiesi, T. Jacobs, C. Maes, and N. S. Skantzos, Phys. Rev. E **74**, 021111 (2006).
[15] F. Bonetto, G. Gallavotti, A. Giuliani, and F. Zamponi, J. Stat. Phys. **123**, 39 (2006).
[16] P. Visco, J. Stat. Mech. (2006) P06006.
[17] K. Saito and A. Dhar, Phys. Rev. Lett. **99**, 180601 (2007).
[18] B. Derrida, J. Stat. Mech. (2007) P07023.
[19] R. J. Harris and G. M. Schütz, J. Stat. Mech. (2007) P07020.
[20] A. Kundu, S. Sabhapandit, and A. Dhar, J. Stat. Mech. (2011) P03007.
[21] K. Saito and A. Dhar, Phys. Rev. E **83**, 041121 (2011).
[22] S. Sabhapandit, Europhys. Lett. **96**, 20005 (2011); Phys. Rev. E **85**, 021108 (2012).
[23] A. Pal and S. Sabhapandit, Phys. Rev. E **87**, 022138 (2013).
[24] Chulan Kwon, Jae Dong Noh, and Hyunggyu Park, Phys. Rev. E **88**, 062102 (2013); Kwangmoo Kim, Chulan Kwon, and Hyunggyu Park, *ibid.* **90**, 032117 (2014).
[25] G. Verley, C. Van den Broeck, and M. Esposito, Phys. Rev. E **88**, 032137 (2013).
[26] G. Verley, C. Van den Broeck, and M. Esposito, New J. Phys. **16**, 095001 (2014).
[27] Alexander K. Hartmann, Phys. Rev. E **89**, 052103 (2014).
[28] A. Crisanti, A. Puglisi, and D. Villamaina, Phys. Rev. E **85**, 061127 (2012).
[29] G. M. Wang, E. M. Sevick, E. Mittag, D. J. Searles, and D. J. Evans, Phys. Rev. Lett. **89**, 050601 (2002).
[30] G. M. Wang, J. C. Reid, D. M. Carberry, D. R. M. Williams, E. M. Sevick, and D. J. Evans, Phys. Rev. E **71**, 046142 (2005).
[31] D. M. Carberry, J. C. Reid, G. M. Wang, E. M. Sevick, D. J. Searles, and D. J. Evans, Phys. Rev. Lett. **92**, 140601 (2004).
[32] W. I. Goldburg, Y. Y. Goldschmidt, and H. Kellay, Phys. Rev. Lett. **87**, 245502 (2001).
[33] J. Liphardt, S. Dumont, S. B. Smith, I. Tinoco Jr., and C. Bustamante, Science **296**, 1832 (2002).
[34] D. Collin, F. Ritort, C. Jarzynski, S. B. Smith, I. Tinoco Jr., and C. Bustamante, Nature (London) **437**, 231 (2005).
[35] S. Majumdar and A. K. Sood, Phys. Rev. Lett. **101**, 078301 (2008).
[36] F. Douarche, S. Joubaud, N. B. Garnier, A. Petrosyan, and S. Ciliberto, Phys. Rev. Lett. **97**, 140603 (2006).
[37] S. Ciliberto, S. Joubaud, and A. Petrosyan, J. Stat. Mech. (2010) P12003.
[38] J. R. Gomez-Solano, A. Petrosyan, and S. Ciliberto, Phys. Rev. Lett. **106**, 200602 (2011).
[39] S. Ciliberto, R. Gomez-Solano, and A. Petrosyan, Annu. Rev. Condens. Matter Phys. **4**, 235 (2013).
[40] J. R. Gomez-Solano, L. Bellon, A. Petrosyan, and S. Ciliberto, Europhys. Lett. **89**, 60003 (2010).
[41] Hugo Touchette, Phys. Rep. **478**, 1 (2009).
[42] K. Sekimoto, Prog. Theor. Phys. Suppl. **130**, 17 (1998); *Stochastic Energetics* (Springer-Verlag, Berlin, 2010).
[43] B. Derrida and E. Brunet, *Einstein Aujourd'hui* (EDP Sciences, Les Ulis, 2005).